Study of the Kinetics of Step and Flash Imprint Lithography Photopolymerization

Michael D. Dickey, Ryan L. Burns, E. K. Kim, Steve C. Johnson, Nick A. Stacey, and C. Grant Willson
The University of Texas, Austin, TX 78712

DOI 10.1002/aic.10477
Published online June 22, 2005 in Wiley InterScience (www.interscience.wiley.com).

Step and Flash Imprint Lithography (SFIL) is a promising high-resolution, yet low-cost patterning technique that uses a UV induced photopolymerization to replicate features on a patterned template. The SFIL process utilizes an acrylate-based free radical polymerization, which is inhibited by oxygen. A semiempirical kinetic model is presented that demonstrates the effects of oxygen on SFIL. On the basis of kinetic measurements, dissolved oxygen causes an inhibition period at the onset of exposure that extends the required exposure time. Oxygen inhibition also results in a thin perimeter of under-cured material surrounding the template due to oxygen diffusion from the ambient during polymerization. The model allows us to study the impact of oxygen on SFIL as a function of various formulation and exposure variables. Methods of limiting the impact of oxygen are presented, such as alternative chemistries and inerting techniques. © 2005 American Institute of Chemical Engineers *AIChE J,* 51: 2547–2555, 2005
Keywords: nanoimprint lithography, reaction kinetics, photopolymerization

Introduction

Photolithography is the cornerstone technology that has enabled the microelectronics industry to print ever-smaller electronic components. As economic forces drive the semiconductor industry toward increasingly smaller feature sizes, technical challenges have led to an exponential growth in the cost of lithographic tools. Imprint lithography offers a high resolution, yet low cost alternative to conventional lithography by avoiding the use of expensive projection optics.[1,2]

Several variations of imprint lithography have been investigated.[3–5] Step and Flash Imprint Lithography (SFIL), depicted in Figure 1, is distinguished by its use of UV curable materials that allow pattern replication at room-temperature and low-pressure.[6,7] SFIL utilizes an acrylate-based, free-radical photopolymerization of the sort found in many industrial applications, such as coatings. Acrylate systems are attractive due to their high reactivity and commercial availability. Unfortunately, oxygen strongly inhibits free radical polymerizations[8] due to its triplet diradical electronic ground state, which is highly reactive toward carbon based radicals.[9] In SFIL, photoinitiated radicals react with oxygen to form peroxy radicals that do not promote acrylate chain growth. Radicals react preferentially with oxygen over monomer, which implies that essentially all dissolved oxygen must be consumed before the system begins to polymerize.[8] Decker provides an excellent summary of the effects of oxygen on acrylate polymerizations.[10] Several studies have been performed on oxygen inhibition, but the effects of oxygen are still being investigated due to the importance of free-radical polymerizations.[11–14]

Since acrylates are often used for coatings, oxygen inhibition has primarily been studied in thin films.[10,12] When thin films are photo cured in an ambient atmosphere, the polymerization in the top few microns of the film is inhibited by diffusing oxygen. This inhibition can alter certain physical properties of the film, such as the modulus at the film's surface.[12] In the SFIL process, the top surface of the film is protected from oxygen diffusion by the quartz template. Despite this protection, oxygen inhibition still presents problems for the SFIL process. Oxygen dissolved in the etch barrier produces an initial inhibition period during irradiation, which ultimately lowers process throughput. In addition, oxygen can diffuse into the etch

Correspondence concerning this article should be addressed to C. G. Willson at willson@che.utexas.edu.

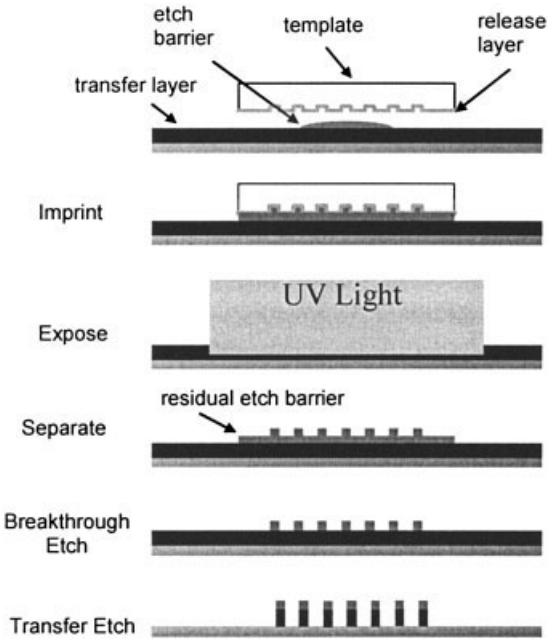

Figure 1. The SFIL process.

barrier from the template edge during curing, as shown in Figure 2a. As a result, a thin layer of under-cured etch barrier surrounds the edges of the imprint, as shown in Figure 2b. This undercured material may potentially foul the template and contribute to defect generation during subsequent imprints. The potential deleterious effects of oxygen on the SFIL process are a focus of this article. Both kinetic measurements and a kinetic-based model of the SFIL are presented.

Materials and Methods

The formulation of the etch barrier was carefully chosen to meet all SFIL processing requirements. For example, the etch barrier must adhere to the transfer layer, but release from the template.[15] Furthermore, the etch barrier must provide sufficient etch resistance and selectivity for the transfer etch.[1] To achieve this end, the etch barrier must contain a minimum of 12 wt. % silicon to provide resistance to an anisotropic oxygen etch.[16] The etch barrier must also have a sufficiently low viscosity to rapidly achieve a thin residual layer during imprinting. The formulation of the etch barrier is a work in progress, but currently a mixture made of four different components is utilized,[1] as seen in Table 1. The total density of the etch barrier solution is 0.92 g/mL at room-temperature, which gives 5.3 mol/L of reactive acrylate groups and 0.061 mol/L initiator (for 1 wt. % initiator) in the etch barrier formulation.

Acrylate monomers are typically used with a benzoin photoinitiator, which undergoes a rapid hemolytic cleavage upon UV exposure, according to a Norrish-type I mechanism, to generate free radicals that initiate the polymerization.[10] Darocur 1173 (2,2-dimethyl 2-hydroxyacetophenone, CIBA) was chosen as the free radical initiator, because it is a commercially available liquid initiator that is both highly efficient,[17] and UV sensitive at 365 nm.

Real Time-Fourier transform infrared (RTIR) spectroscopy was used to monitor the polymerization. RTIR utilizes *in situ* IR measurements to track the disappearance of acrylate double bonds during photo curing.[10] A Nicolet Magna-IR 550 was used at 8 cm^{-1} resolution, which allowed for measurements every 0.07 s. Samples were prepared by placing a drop of etch barrier solution on a double polished silicon wafer. The drop was covered with a sodium chloride disk (Wilmad). The salt disk forced the drop to form a thin film and provided a barrier to prevent oxygen diffusion during curing. Dissolved oxygen was not removed from the etch barrier. Monomer was used as received: TBA (98%, Aldrich 327182), EGDA (96%, Aldrich 409995), and SIA (Gelest SIA 0210.0).

Each monomer contains a low concentration of MEHQ (Hydroquinone monomethyl ether) that is added by the manufacturer to provide stability during shipping. It was experimentally determined that removing the MEHQ inhibitor resulted in no observable difference in the kinetics. To prove this claim, the inhibitor was removed from each component using commercially available inhibitor removal columns (Aldrich 306312). The polymerizations were irradiated with a mercury lamp (Novacure EFOS) at 31.8 mW/cm^2, unless otherwise noted. The polymerizations were all performed under normal, ambient atmospheric conditions.

The properties of oxygen in the etch barrier are critical to the kinetic model. The initial concentration of dissolved oxygen in the etch barrier was 2.8×10^{-4} mol/L, as measured using a dissolved oxygen probe (YSI-5100). Generally, acrylate systems are assumed to contain 10^{-3} mol/L oxygen,[18] but this appears to be a literature estimate rather than a measured value. The diffusion coefficient of oxygen in the etch barrier was measured as 5.5×10^{-6} cm^2/s. The diffusivity of oxygen in the monomer solution was measured using chronoamperometry,[19] a method that relies on measuring both the transient and steady state current resulting from oxidation of diffusing oxygen to an electrode of known diameter (25 μm, platinum) submerged in solution.

Kinetics Background

Classical free radical polymerization kinetics[20] were assumed to give a first-order approximation of the effects of oxygen. This model consists of four important reaction steps: initiation, propagation, termination, and radical scavenging, as shown as follows.

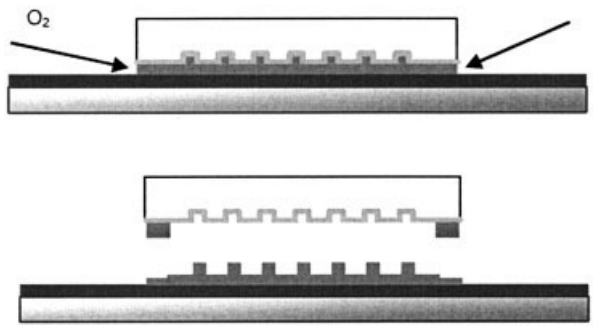

Figure 2. (a) Oxygen diffuses into the perimeter of the etch barrier under the template. (b) Undercured material remains on template, potentially affecting subsequent imprints.

Table 1. Etch Barrier Composition

Component	Structure	Purpose	Weight Percent
Gelest SIA-0210 (SIA)	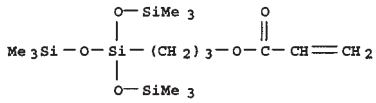	Silicon containing monoacrylate for etch resistance	44
Ethylene Glycol Diacrylate (EGDA)	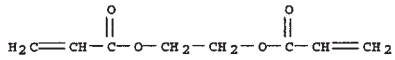	Crosslinker for mechanical stability	15
t-Butyl Acrylate (TBA)	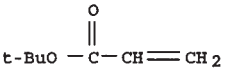	Reactive diluent to maintain low viscosity	37
Darocur 1173	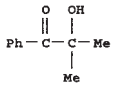	Photoinitiator	1–4

Initiation: $I + h\upsilon \rightarrow 2R$

Radical Scavenging: $R + O_2 \rightarrow$ stable peroxy radical

Polymerization: $M + R \rightarrow MR$

$M_nR + M \rightarrow M_{n+1}R$

Termination: $M_nR + M_mR \rightarrow M_{n+m}$ (combination)

$M_nR + M_mR \rightarrow M_n + M_m$ (disproportionation)

I, R, O_2, M, and M_nR represent, respectively, initiator, radicals, oxygen, acrylate monomer, and radical chains of length n. M_{n+m} represents the polymer that results from termination. The initiation step involves an initiating species absorbing UV light, $h\upsilon$, and splitting into two radicals. Generated radicals rapidly react with oxygen to form peroxy species that are nonreactive towards the acrylate double bond, but once the oxygen is depleted, the radicals react with monomer to form a growing polymer chain. It has been shown experimentally that the concentration of dissolved oxygen must be lowered by at least two-orders of magnitude before polymerization begins, due to the high reactivity of oxygen with radicals.[8] The polymer chain continues to propagate until it encounters a radical end of another chain at which point the two radical ends terminate by either combination or disproportionation.

The critical rate equations for the model include the rate of initiation, radical scavenging, polymerization, and termination. The expression for rate of initiation is shown in Eq. 1. In Equations 1–4, the brackets ([. . .]) denote concentration (mol/L).

$$\text{Rate of Initiation:} \qquad R_i = 2\Phi k_I[I] \tag{1}$$

R_i is the rate of initiation, and k_I is the reaction coefficient for initiation (s^{-1}), which represents the amount of light absorbed per mol of initiator. Equation 1 has a coefficient of 2, due to two radicals formed for each initiator broken down. We define the quantum yield Φ, as the product of two terms $\Phi = \Phi' f$, where f is the initiator efficiency (fraction of radicals produced that initiate propagating chains), and Φ' is the number of initiator molecules dissociated per photon absorbed.[8,21] The notation of Eq. 1 was chosen such that the effects of initiator absorbance and irradiation intensity can be wrapped into one term k_I, which is useful when modeling the effects of initiation on the polymerization. Following the initiation step, radicals that react with oxygen form relatively stable peroxy radicals. The kinetic rate expression is shown in Eq. 2.

$$\text{Rate of Scavenging:} \qquad R_{O2} = -k_o[O_2][R] \tag{2}$$

Here k_o is the rate coefficient of oxygen consumption (L/mol · s). On the basis of previous studies, the value of k_o was assumed to be 1×10^9 (L/mol · s).[8,22,23] This value is several orders of magnitude higher than any other reaction coefficients in the polymerization. Due to the large difference in reactivity, essentially no polymerization occurs in the presence of oxygen. Equation 2 implies that one radical consumes one oxygen molecule. In certain reaction systems, a single radical is often capable of consuming multiple oxygen molecules since the peroxy radical can generate new radicals via hydrogen abstraction.[13] However, the SFIL acrylate formulation does not contain any easily abstractable hydrogens. Once the concentration of oxygen is sufficiently reduced, the radicals begin to react with monomer to form polymer. The kinetic expression for polymerization is shown in Eq. 3

$$\text{Rate of Polymerization:} \qquad R_p = -k_p[M][R] \tag{3}$$

R_p is the rate of polymerization, and k_p is the rate coefficient of polymerization (L/mol · s). By definition, the rate of polymerization is the rate at which monomer is consumed. Individual radical chains continue to propagate until they are terminated by another radical. The kinetics of the termination process is shown in Eq. 4.

$$\text{Rate of Termination:} \qquad R_t = -2k_t[R][R] \tag{4}$$

Here k_t represents the termination coefficient (L/mol · s), which generically represents the combined effects of combination and

disproportionation. The factor of 2 accounts for two radical chains destroyed per termination event. It should be noted that $[R]$ represents the concentration of all radicals, regardless of chain length (that is, M_nR). This is a classic assumption that simplifies the modeling tremendously. This assumption is generally justified by considering the rate coefficients k_p and k_t to represent the net effect of polymerization and termination processes. Furthermore, k_p and k_t are coefficients, not constants, and subsequently change as the reaction proceeds. This approach helps to account for chain length dependent reactions[24,25] and changes in the reaction medium due to polymerization.

A species balance based on Eqs. 1–4 gives the basis for the following kinetic expressions

$$\text{Initiator:} \quad \frac{d[I]}{dt} = -\Phi' k_I[I] \tag{5}$$

$$\text{Radicals:} \quad \frac{d[R]}{dt} = 2\Phi k_I[I] - k_o[O_2][R] - 2k_t[R]^2 \tag{6}$$

$$\text{Oxygen:} \quad \frac{d[O_2]}{dt} = D_{O_2}\frac{\partial^2[O_2]}{\partial x^2} - k_o[O_2][R] \tag{7}$$

$$\text{Monomer:} \quad \frac{d[M]}{dt} = -k_p[M][R] \tag{8}$$

Equation 7 contains the oxygen diffusion coefficient, D (cm^2/s). This expression for diffusion, based on Fick's second law, accounts for diffusion of oxygen from the perimeter of the template. It should be further noted that the etch barrier is a ternary system, so the reaction coefficients are overall coefficients representing the net effect of the system. The values of the reaction coefficients in Eqs. 5–8 were measured as described in an accompanying article.[26]

Equation 8, which is the expression for the rate of polymerization, is in terms of both monomer and radical concentration. Radical concentration is very difficult to measure experimentally, thus, it is common practice to utilize an alternative expression for radicals. A more convenient expression for the rate of polymerization can be obtained by applying the well known quasi steady-state approximation (QSSA), which assumes the rate of initiation is equal to the rate of termination.[20] The QSSA is reasonable when the radical lifetimes are small compared to the time scales of initiator consumption and monomer conversion. Making the QSSA gives the following expression for the rate of polymerization, as seen in Eq. 9. This expression is experimentally useful since all terms in Eq. 9 are measurable

$$\frac{d[M]}{dt} = -k_p[M]\left(\frac{R_i}{2k_t}\right)^{0.5} \tag{9}$$

The power of 0.5 in Eq. 9 is highly dependent on the termination mechanism. This coefficient is referred to as alpha (α), and is exactly 0.5 when the radicals terminate entirely by the classical bimolecular mechanism. When primary radical termination (PRT) occurs, α drops below 0.5.[27] PRT is a termination process whereby primary radicals scavenge growing radicals chains rather than reacting with monomer to form a polymer chain. Primary radicals are either initiated radicals or short chain radicals that have high mobility compared to long radical chains. Equation 9 holds well for most systems since PRT usually only occurs when there is a large concentration of radicals compared to monomer groups.[28] Similarly, unimolecular termination has the effect of raising α above 0.5. Unimolecular termination results when radical chains become trapped within the polymer matrix and are unable to terminate in a bimolecular reaction. Therefore, α is expected to increase with conversion as unimolecular termination becomes more prominent due to gelation. This is especially true in multifunctional systems where crosslinking limits mobility. For instance, α has been shown to be ~0.85 in a multifunctional acrylate system, implying unimolecular termination.[29] In order to use classical kinetic modeling, α must be ~0.5. Thus, we set out to determine α for the SFIL etch barrier system to learn more about the termination mechanisms at play and to determine the applicability of Eq. 9 for further kinetic analysis.

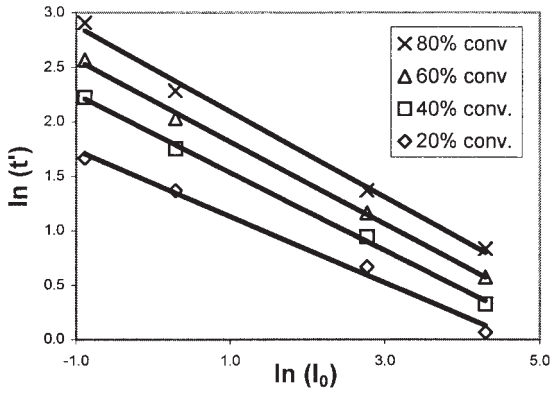

Figure 3. Determination of α for a 4 wt % Darocur 1173 system (the slope is equivalent to Alpha, as measured at various conversions).

Results

Determining alpha

An established method was used to determine α for the etch barrier acrylate system.[27] Etch barrier with 4 wt. % initiator loading was exposed at various intensities and RTIR was used to track the disappearance of monomer. The value of α is equivalent to the slope of a plot of $\log(t')$ vs. log(intensity). The t' represents the time to reach a given conversion minus the inhibition time due to inherent oxygen, which does not factor into the analysis. By performing this analysis at various points of conversion, the variation of α with conversion can be determined. The data from this method are shown in Figure 3 and the results summarized in Table 2. The methodology behind the α measurement is partly flawed since changing light intensity can change the radical concentration, and, thus, increase the likelihood of primary radical termination. However, the linear fit of the results and the consistency of the data suggest that the reaction environment is a more important factor than light intensity in determining α. The value of α appears to increase with conversion from ~0.3 to ~0.4 in the etch barrier

Table 2. Summary of α Values for 4 wt. % Dacocur 1173 Taken from Figure 3

Percent Conversion	Alpha	R^2
20	0.31	0.993
40	0.36	0.998
60	0.38	0.998
80	0.39	0.994

R^2 is the correlation coefficient from the linear fit of the data.

Table 3. Alpha (α) using 1 wt. % Darocur 1173

Percent Conversion	Alpha	R^2
10	0.46	0.993
20	0.44	0.977
30	0.43	0.979
40	0.43	0.976
50	0.45	0.967
60	0.46	0.936
70	0.52	0.997

with a 4 wt. % initiator etch barrier system. The increase of α with conversion is consistent with theory since the onset of gelation limits the mobility of small radicals. Generally, free radical formulations use initiator concentrations between 0.5–5 wt. % initiator. It is not surprising that the highend of this scale results in some primary radical termination due to the high concentration of initiator.

Alpha for a 1 wt. % initiator etch barrier formulation was also measured, while keeping the proportions of the other components constant relative to each other. Table 3 shows that α is 0.46 when using 1 wt. % Darocur 1173 in the etch barrier formulation, which is very close to the 0.5 value for pure bimolecular termination using the steady state approximation. The value of α is essentially constant, within experimental error, over the range of conversions studied.

The value of α was also determined using a separate analysis technique.[10] An estimation for α can be made by comparing R_p for polymerizations at different irradiation intensities. The principle behind this method stems from the fact that R_p is proportional to irradiation intensity raised to the power of α. Using this method, α was found to be 0.58 ± 0.08 from 10–50% conversion, with no apparent trend in the data. This slightly larger value of α is likely due to the error associated with determining R_p. These methods each have their limitations, but the results are consistent with the use of the theoretical value of α (0.5) as a first-order approximation in the kinetic modeling.

Of course, the value of α represents the net effect of the termination mechanisms involved in the polymerization. Therefore, in theory a α value of 0.5 could represent a combination of unimolecular, primary radical, and bimolecular termination. To prove that bimolecular termination is the dominant termination mechanism in a system with a α of $\sim$0.5, the absence of either PRT or unimolecular termination must be verified. Previously, the presence of unimolecular termination has been observed in polymer samples by heating crosslinked samples post-photocuring. This heating mobilizes trapped radicals and results in additional observable conversion.[30,31] When cured etch barrier samples were heated, this effect was not observed experimentally, so it was concluded that unimolecular termination is insignificant. It is likely that the termination mechanism is primarily bimolecular since α is close to 0.5, and there are no signs of significant unimolecular termination. Therefore, the use of Eq. 9 is justified in both the kinetic analysis and modeling.

Results

SFIL kinetics

Before analyzing the kinetics of the etch barrier mixture, kinetic profiles of the individual components in the etch barrier were obtained by performing three separate homopolymerizations. As shown in Figure 4, each component has a unique kinetic profile. (Note that the data was taken at 1 mW/cm^2 in order to accentuate the unique aspects of the curing profiles of the components.) The *t*-butyl acrylate component displays autoacceleration, which can be seen as the polymerization rate increases from 10% conversion to 40% conversion. Autoacceleration is a well-known phenomenon that is characterized by an increasing rate of polymerization with conversion. As the polymerization proceeds, the reaction environment grows more viscous and cross-linked, which limits the mobility of radical chains. This causes the radical termination rate to drop and consequently the polymerization rate increases. The *t*-butyl acrylate reaction goes to nearly complete conversion, which indicates that the monomer maintains high mobility up to high conversions, as expected. EGDA cures rapidly at low conversions due its difunctionality, which increases the reactive acrylate group concentration, and also results in crosslinking that contributes to autoacceleration at very low conversions. In contrast to *t*-butyl acrylate, EGDA only partially cures due to cross-linking. Due to its difunctionality, the EGDA monomer can be incorporated into the polymer, while still maintaining an unreacted functional group. SIA also reacts rapidly at low conversions, possibly due to the viscosity of the bulk material ($\sim$3.83 cp), which would limit chain mobility and, thus, lower the rate of termination. The monofunctional SIA goes to nearly complete conversion, which indicates that the monomer maintains high mobility up to high conversions.

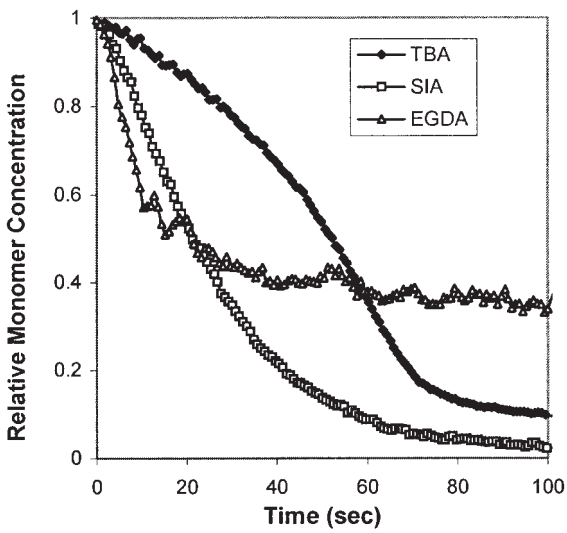

Figure 4. Individual components (1.0 mW/cm^2, 4 wt % Darocur 1173, no oxygen).

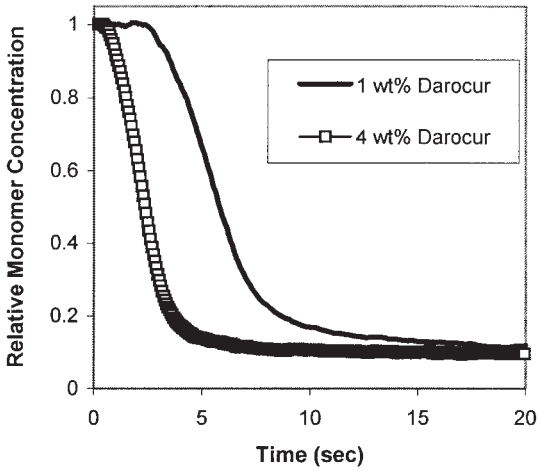

Figure 5. Etch barrier polymerization (31.8 mW/cm^2).

The kinetic profile of the etch barrier is shown in Figure 5 at two initiator concentrations. The inhibition period is four times as long for 1 wt. % initiator as for 4 wt. %, which is in perfect agreement with theory (0.61 s for 4 wt. % and 2.64 s for 1 wt. %, based on the time to reach 1% conversion). Thus, higher initiator concentration provides added benefit for SFIL by reducing the inhibition period, which has literature precedent.[17] There are tradeoffs to increasing the initiator concentration though, such as increasing the optical opacity of the film, which could lead to under cured regions in extreme cases. Furthermore, raising the initiator concentration increases the likelihood of primary radical termination, which lowers the efficiency of the reaction. In systems containing monofunctional monomer, the average polymer chain length is shortened with increased initiator concentration, which would be detrimental to the mechanical properties of the polymer. Although, typical initiator concentrations range from 0.5 to 5 wt. %, an analysis of mechanical properties as a function of initiator concentration is outside the scope of this article.

The data from Figure 5 were analyzed further by finding the relative rate of polymerization (R_p/M_o) as a function of conversion by determining the slope, as shown in Figure 6. The

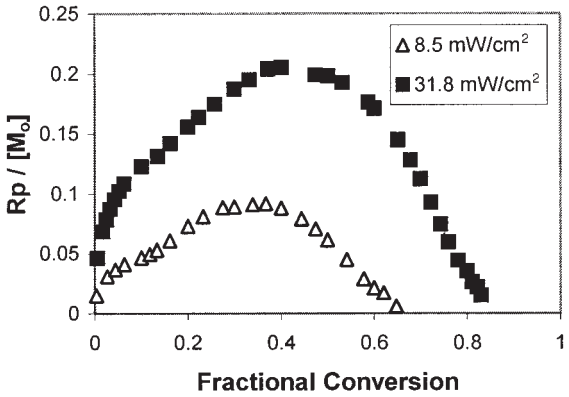

Figure 6. Rate of polymerization analysis for a 1 wt. % Darocur 1173 system at 8.5 and 31.8 mW/cm^2 (R_p/M_o is the rate of polymerization divided by the initial monomer concentration).

Table 4. Initial Conditions for Model

Component	Initial Condition (mol/L)
Monomer	5.3
Initiator	6.0×10^{-2}
Radicals	0
Oxygen	2.80×10^{-4}

rate of polymerization displays the typical characteristics of bulk free radical polymerizations. There is an initial rapid increase in polymerization rate, followed by a more gradual rate increase (autoacceleration), reaching a maximum at ~40% conversion. Many multifunctional polymerization systems reach max R_p at 10–30% conversion.[10] The SFIL etch barrier contains only 15 wt. % crosslinker (EGDA), so it is not surprising that R_p reaches a maximum at slightly higher conversions.

In Figure 6, the higher intensity exposure (31.8 mW/cm^2) has a higher rate of polymerization than the lower intensity (8.5 mW/cm^2), as expected. However, the maximum rate of polymerization occurs at a higher fractional conversion. This is consistent with a theory related to delayed volume shrinkage, which occurs during intense illumination.[32] The principle of this theory is that higher polymerization rates allow less time for volume relaxation, and thus, the reactive components maintain greater mobility up to a higher conversion. Therefore, all studies for the rate coefficients were performed at the same intensity, which was chosen to mimic the exposure source on our SFIL tool.[33] Figure 6 also displays a well-known trend: high light intensities lead to higher final conversion. Again, this is likely due to a temporary excess free volume, which occurs due to the volume shrinkage rate lagging behind the reaction rate.[31,34] Of course, the final conversion is normally found to be less than 100% due to diffusional constraints.[34]

Results

SFIL modeling

The reaction kinetics were modeled using Eqs. 5–8 in MATLAB.® Use of these equations requires knowledge of the reaction coefficient values. It should be noted that values of the coefficients k_p and k_t are dependent on conversion since molecular mobility in the reaction medium decreases as the polymerization proceeds. In particular, k_t is highly dependent on conversion since the termination process is diffusion controlled.[35] Consequently, effects, such as autoacceleration and autodeceleration can only be accounted for by measuring these coefficients as functions of conversion. Measuring the reaction coefficients is not a trivial task, and is presented in an accompanying article.[26] Use of Eqs. 5–8 also requires knowledge of the initial conditions, which are listed in Table 4.

Combining the initial conditions and the measured reaction coefficients allows the use of Eqs. 5–8 in a predictive computer based model to show the effects of oxygen on the polymerization process. First, the accuracy of the measured coefficients was validated by comparing the output of the model with experimental data, as seen in Figure 7. Figure 7 is a one-dimensional (1-D) model, thus, does not incorporate the diffusivity of oxygen. The initiator efficiency was assumed constant through 80% conversions, at which point it was forced to decay exponentially to reflect the limiting effects of vitrification on

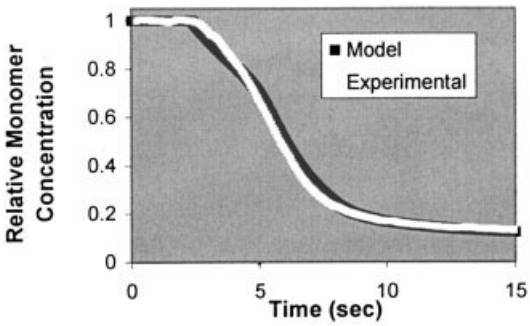

Figure 7. Comparison of model vs. experimental data (1 wt. % Darocur 1173, 31.8 mW/cm^2).

conversion observed experimentally. The model agrees well with the experimental data. The largest deviation is at the beginning of the polymerization (up to 20% conversion), where rate coefficients are the most difficult to measure due to the rapid rate of polymerization.

Once the validity of the kinetic aspects of the model were verified against experimental data, the effect of oxygen diffusion was incorporated into the model, which requires two boundary conditions. Boundary conditions were applied at the edge of the template and in the middle of the template. Oxygen was assumed to remain saturated at the edge of the template. Similarly, the oxygen concentration was assumed not to have a gradient under the middle of the template due to symmetry. Of the four components tracked in the model (monomer, initiator, radials, and oxygen), oxygen was the only component assumed to have significant diffusion. There are no gradients in the initiator concentration since the irradiation is uniform across a thin film. Radicals are assumed to not diffuse significantly compared to oxygen because of their reactivity with monomer and other radicals.[36] Once the inherent dissolved oxygen is consumed in the initial stages of the reaction, there become essentially two "regions" under the template. An interior region devoid of significant oxygen, which polymerizes rapidly, and a perimeter region containing oxygen diffusing from the ambient, which essentially does not polymerize due to the reactivity of oxygen with free radicals. In the polymer-containing region, diffusion is likely to be very slow due to high viscosity and chain entanglements. In the oxygen-containing perimeter, there is essentially no monomer gradient because no polymerization takes place due to oxygen inhibition. Assuming a constant diffusivity for oxygen provides a worse case scenario since there is likely to be some polymerization in the perimeter region. Oxygen diffusivity has been shown to be at least two orders of magnitude lower in a polymer matrix, which is an approximation based on oxygen induced scavenging.[36]

The results of the model that incorporate oxygen diffusion are shown in Figure 8. The axis labeled time represents the duration of UV irradiation, with time zero indicating the beginning of irradiation. The axis labeled distance represents the distance into the etch barrier with respect to the edge of the template. A distance of zero marks the edge of the etch barrier, which is exposed to ambient oxygen. Only the outer 80 microns of the etch barrier are shown in this model because diffusing oxygen only affects the perimeter of the etch barrier. The polymerization in the interior, which is immune to the diffusional effects of oxygen, is represented by the profile of a

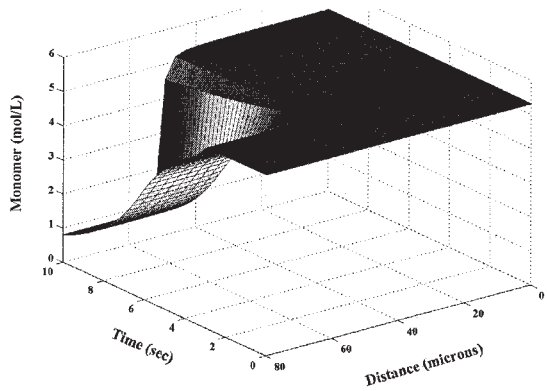

Figure 8. Time-spatial model of etch barrier polymerization including the effects of diffusing oxygen (1 wt. % initiator, 31.8 mW/cm^2).

planar cross-section at 80 microns. This profile is identical to the results of Figure 7, where diffusional effects were neglected.

Two distinct effects of oxygen are revealed and quantified in Figure 8. First, the inhibition period due to dissolved oxygen is shown during the first few seconds of irradiation. Essentially no polymerization takes place in the presence of oxygen, which demonstrates the inhibitory strength of the oxygen. This is best illustrated in Figure 7, where the inhibition period is shown to be 2.3 s for the formulation and exposure conditions. The second distinct feature of Figure 8 is the effect of diffusing oxygen, which inhibits polymerization on the perimeter of the etch barrier. A snapshot of the monomer profile after 10 s of irradiation best illustrates this phenomenon, as shown in Figure 9.

On the basis of the model, oxygen diffusion results in an undercured layer of about 50 μm around the etch barrier perimeter, as seen in Figure 9. This phenomenon has been observed experimentally, but is difficult to quantify. A crude calculation using a diffusion coefficient between 10^{-5} and 10^{-6} cm^2/s of oxygen in monomer gives a diffusion length estimated to be 2–140 μm based on diffusion theory, assuming a 10 s reaction time.[12] The diffusion length calculated from the model is in the middle of this range, which shows that the value is reasonable. The steepness of the monomer profile in Figure

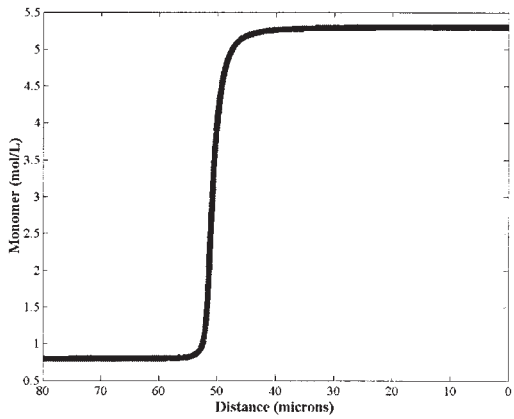

Figure 9. Etch barrier polymerization at 10 s (1 wt. % initiator, 31.8 mW/cm^2).

9 is due to the magnitude of the oxygen reaction coefficient. The implication is that in the presence of even a small amount of oxygen, no polymerization occurs, but in the absence of oxygen, polymerization proceeds rapidly. The model provides a worst-case scenario for the length of the undercured boundary because it assumes constant oxygen diffusivity throughout the polymerization. The effects of oxygen are retarded by increases in viscosity and can be extremely restricted in the vitrified state.[37] However, due to the high reactivity of oxygen with radicals, it is unlikely that any significant polymerization occurs in the presence of oxygen, so the assumption of constant diffusivity is reasonable. By increasing the initiator concentration to 4 wt. % and using a more intense mercury lamp of 43 mW/cm^2, the undercured layer is reduced to $\sim$22 μm according to the model. Similarly, a change of this nature would reduce to inhibition time from 2.3 s to approximately 480 ms.

There are a number of factors that influence the inhibitory effect of oxygen including the diffusivity of oxygen, the photoinitiator absorbance and efficiency, and the irradiation intensity.[10] The last two factors are accounted for by the product $\Phi \cdot k_I$. Thus, by increasing the value of $\Phi \cdot k_I$, the deleterious effects of oxygen are reduced. However, the rate of polymerization can actually reach a maximum at extreme light intensities, which is called the saturation point. This has been reported to occur at $\sim$100 mW/cm^2.[17,38] It is possible that this maximization is due to the onset of primary radical termination, which negates the benefits of creating additional radicals. In addition to increasing the irradiation intensity, the product $\Phi \cdot k_I$ can be increased by considering alternative initiators. For example, Irgacure 369 has been shown to reduce the effects of oxygen, presumably due to its high efficiency.[14]

Increasing k_I is one of several options available to reduce the effects of oxygen. One obvious option is to remove the dissolved oxygen prior to polymerization. A 10-min nitrogen flush has proven sufficient to get rid of oxygen.[32] For short degassing periods, helium was found to be more effective than nitrogen, due to the relative size of the molecules.[39] An inert gas flush is not an ideal option for SFIL because it would likely change the composition of the etch barrier due to differences in component volatility. As an alternative, the dissolved oxygen could be removed by a pump/freeze/thaw method, but this is also an inefficient alternative for this application. Even if oxygen was removed from the etch barrier prior to polymerization, oxygen would also have to be removed from the imprinting area by an inert blanket to eliminate diffusion effects. Carbon dioxide is an advantageous inert blanket since it is heavier than air, which results in a pooling effect.[10,13,14] A blanketing system would inevitably increase operating costs.

Several additives have been proposed to overcome the effects of oxygen, such as amines and thiols. Amines bind oxygen, while yielding radicals capable of contributing to the polymerization.[12] For instance, cyclic N-vinylamides were used to increase the rate of polymerization in systems exposed to air, although the mechanism is still unclear.[9] Aromatic thiols have been shown to aid polymerization by rejuvenating peroxy radicals.[18] However, none of these systems have proven to be robust, and furthermore thiols are not a feasible option for the material sensitive semiconductor industry. Amines are particularly troublesome to the base sensitive imaging processes used in the microelectronics industry.

There are several alternative polymerization chemistries, such as the polyene–thiol systems, which are insensitive to oxygen but obviously contain a thiol component.[10] Similarly, cationic polymerizations are not inhibited by oxygen.[40] Cationic polymerizations benefit from a post-polymerization period in the dark, low shrinkage, high mechanical performance, and good adhesion. Results of this study have led our group to pursue cationic polymerization etch barrier systems and preliminary results are very promising.[41]

Conclusions

A model has been developed to quantify the inhibitory effects of oxygen on the SFIL etch barrier polymerization. An analysis of the kinetics verified the validity of equations used in the model and illustrated that the termination mechanism is primarily bimolecular by showing α to be $\sim$0.5. A significant inhibition period was shown to result from dissolved oxygen in the etch barrier depending on the irradiation intensity and initiator concentration. The etch barrier perimeter, which is exposed to ambient oxygen, is inhibited by diffusing oxygen. This results in a ring of undercured etch barrier around the perimeter of the template for reasonable exposure conditions (4 wt. % initiator with 43 mW/cm^2). A predictive model was presented that shows the effects of changing the initiation conditions on oxygen diffusion length. Methods are available to reduce or even overcome the effects of oxygen and they are being pursued in our group.

Acknowledgments

We thank the NSF for a fellowship for Michael Dickey and DARPA for funding, contract N66001-01-1-8964. We appreciate the value discussion with Dr. John Ekerdt, Dr. Bonnecaze, and Dr. Nick Stacey. We thank Zach Hilt of the Peppas research group with help measuring the dissolved oxygen content and Dr. Bob LeSeur of the Bard research group for assistance with the oxygen diffusion chronoamperometry measurements. We are also grateful for contributions by Justin Shih.

Literature Cited

1. Johnson SC, Bailey TC, Dickey MD, Smith BJ, Kim EK, Jamieson AT, Stacey NA, Ekerdt JG, Willson CG, Mancini DP, Dauksher WJ, Nordquist KJ, Resnick DJ. *Proceedings of SPIE—The International Society for Optical Engineering* 2003;5037:197–202.
2. *International Technology Roadmap for Semiconductors;* Semiconductor Industry Association: San Jose; CA, 2003.
3. Colburn M, Johnson S, Stewart M, Damle S, Bailey TC, Choi B, Wedlake M, Michaelson T, Sreenivasan SV, Ekerdt J, Willson CG. *Proceedings of SPIE—The International Society for Optical Engineering* 1999;3676:379–389.
4. Chou SY, Krauss PR, Zhang W, Guo L, Zhuang L. Microelectronics and nanometer structures. *J of Vacuum Sci & Technol B* 1997;15: 2897–2904.
5. Whidden TK, Ferry DK, Kozicki MN, Kim E, Kumar A, Wilbur J, Whitesides GM. Pattern transfer to silicon by microcontact printing and RIE step and flash imprint lithography: defect analysis. *Nanotechnology.* 1996;7:447–451.
6. Bailey TC, Johnson SC, Sreenivasan SV, Ekerdt JG, Willson CG, Resnick DJ. Step and flash imprint lithography: an efficient nanoscale printing technology. *J of Photopolymer Sci and Technol.* 2002;15: 481–486.
7. Bailey T, Smith B, Choi BJ, Colburn M, Meissl M, Sreenivasan SV, Ekerdt JG, Willson CG. Step and flash imprint lithography: defect analysis. Microelectronics and Nanometer Structures. *J of Vacuum Sci & Technol, B* 2001;19:2806–2810.
8. Decker C, Jenkins AD. Kinetic approach of oxygen inhibition in ultraviolet- and laser-induced polymerizations. *Macromolecules.* 1985;18:1241–1244.

9. Miller CW, Hoyle CE, Jonsson S, Nason C, Lee TY, Kuang WF, Viswanathan K. *ACS Symposium Series*. Chicago, IL. 2003;847:2–14.
10. Decker C. *Macromolecular Rapid Communications.* 2002;23:1067–1093.
11. Decker C. *Polymer International* 1998;45:133–141.
12. Cao H, Currie E, Tilley M, Jean YC. ACS Symposium Series 2003; 847:152–164.
13. Studer K, Decker C, Beck E, Schwalm R. *Progress in Organic Coatings* 2003;48:92–100.
14. Studer K, Decker C, Beck E, Schwalm R. *Progress in Organic Coatings* 2003;48:101–111.
15. Bailey T, Choi BJ, Colburn M, Meissl M, Shaya S, Ekerdt JG, Sreenivasan SV, Willson CG. Microelectronics and nanometer structures. *J of Vacuum Sci & Technol B* 2000;18:3572–3577.
16. Colburn M, Grot A, Amistoso MN, Choi BJ, Bailey TC, Ekerdt JG, Sreenivasan SV, Hollenhorst J, Willson CG. *Proceedings of SPIE—The International Society for Optical Engineering* 2000;3997:453–457.
17. Decker C, Moussa K. *Makromolekulare Chemie* 1990;191:963–979.
18. Krongauz VV, Chawla CP. *Abstracts of Papers, 222nd ACS National Meeting, Chicago, IL, United States,* August 26–30; 2001;POLY-376.
19. Bard AJ, Faulkner LR. *Electrochemical methods: fundamentals and applications.* 2nd ed. Wiley: New York; 2001.
20. Odian GG. *Principles of polymerization.* 3rd ed. Wiley: New York: 1991.
21. Kurdikar DL, Peppas NA. Kinetics of photopolymerization of multifunctional monomers. *Polymeric Materials Sci and Eng* 1993;69:174–175.
22. Fouassier JP, Merlin A. Laser investigation of Norrish type I photoscission in the photoinitiator Irgacure (2,2-dimethoxy-2-phenylacetophenone). *J of Photochem* 1980;12:17–23.
23. Neta P, Huie RE, Ross AB. Rate constants for reactions of peroxyl radicals in fluid solutions. *J of Physical and Chem Ref Data* 1990;19: 413–513.
24. Berchtold KA, Lovell LG, Nie J, Hacioglu B, Bowman CN. *Polymer* 2001;42:4925–4929.
25. Hacioglu B, Berchtold KA, Lovell LG, Nie J, Bowman CN. *Biomaterials* 2002;23:4057–4064.
26. Dickey MD, Willson CG. *AIChE J* Submitted.
27. Bajdala J, Mueller U, Wartewig S, Winkler K. Photoinitiated crosslinking of silicones. 10. Photoinitiated crosslinking of silicone acrylates as studied by Fourier transform infrared spectroscopy. *Makromolekulare Chemie* 1993;194:3093–3105.
28. Goodner MD, Bowman CN. Modeling primary radical termination and its effects on autoacceleration in photopolymerization kinetics. *Macromolecules* 1999;32:6552–6559.
29. Decker C. *ACS Symposium Series.* 1984;266:207–223.
30. Decker C, Moussa K. Laser-induced polymerization. *J of Polymer Sci., Part A: Polymer Chemistry.* 1987;25:739–742.
31. Kloosterboer JG, Van de Hei GMM, Gossink RG, Dortant GCM. *Polymer Communications.* 1984;25:322–325.
32. Anseth KS, Wang CM, Bowman CN. *Polymer.* 1994;35:3243–3250.
33. Choi BJ, Johnson SC, Sreenivasan SV, Colburn M, Bailey TC, Willson CG. Partially constrained compliant stages for high resolution imprint litography. *Proc. ASME DETC2000,* 2000;861.
34. Kurdikar DL, Peppas NA. *Vysokomolekulyarnye Soedineniya, Seriya A i Seriya B.* 1994;36:1852–1861.
35. Buback M, Egorov M, Gilbert RG, Kaminsky V, Olaj OF, Russell GT, Vana P, Zifferer G. *Macromolecular Chemistry and Physics.* 2002; 203:2570–2582.
36. Krongauz VV, Schmelzer ER, Yohannan RM. *Polymer.* 1991;32: 1654–1662.
37. Andrzejewska E. Photopolymerization kinetics of multifunctional monomers. *Progress in Polymer Sci.* 2001;26:605–665.
38. Okamura S, Manabe T. Radiation polymerization in solution. III. Effect of primary radicals in the termination reaction. *Polymer.* 1961; 2:83–94.
39. Krongauz VV, Chawla CP, Dupre J. Kinetics of anisotropic photopolymerization in polymer matrix. *ACS Symposium Series.* 2003;847: 165–175.
40. Decker C. Light-induced crosslinking polymerization. *Polymer International.* 2002;51:1141–1150.
41. Kim EK, Stacey NA, Smith BJ, Dickey MD, Johnson SC, Trinque BC, Willson CG. Microelectronics and nanometer structures—Processing, measurement, and phenomena. *J of Vacuum Sci. & Technol, B.* 2004; 22:131–135.

Manuscript received July 19, 2004, and revision received Dec. 7, 2004.